

## DAILY PERFORMANCE EVALUATION OF A TROMBE-MICHEL WALL

### Daniel Sampaio Figueira

Centro Federal de Educação Tecnológica do Paraná - Via do Conhecimento km 01, Caixa Postal 571, 85501-970, Pato Branco, Pr.  
E-mail: [dfigueira@cpovo.net](mailto:dfigueira@cpovo.net)

### Arno Krenzinger

Univ. Federal do Rio Grande do Sul, Depto Engenharia de Materiais – Osvaldo Aranha, 99/ 711, 90035-190, Porto Alegre, R.S.  
E-mail: [arno@mecanica.ufrgs.br](mailto:arno@mecanica.ufrgs.br)

### Horacio Antonio Vielmo

Univ. Federal do Rio Grande do Sul, Depto Engenharia Mecânica - Sarmento Leite, 425, 90050-170, Porto Alegre, R.S. E-mail:  
[vielmoh@mecanica.ufrgs.br](mailto:vielmoh@mecanica.ufrgs.br)

**Abstract.** This paper presents a method for evaluating the daily performance of a truncated Trombe-Michel wall. Trombe-Michel wall is a system that uses solar energy to improve the thermal comfort of a building. In order to reduce the number of involved variables a section of the wall was thermally insulated with a 1.96 m (width) x 1.45 m (height) x 1.10 m (depth) box made of expanded polystyrene 50 mm thick sheets. Plastic bottles filled with water, acting as a thermal storage mass, were symmetrically arranged inside the box. For temperature and irradiance measurements, a data acquisition unit interfaced to a computer was employed. Temperatures were sensed by 22 integrated circuit sensors and 8 platinum resistance sensors measured in a 4-wire configuration. Two photovoltaic sensors were used for irradiance measurements. The characterization of the system was obtained through the determination of the transmittance of the coverings, delay in the heat peak and the daily efficiency. The transmittance of the double glazed cover reaches approximately 55 %. There is a 4-5 hours delay in the supplying of heat by the wall. The determined daily efficiency fluctuated between 15 % to 25 %.

**Keywords.** Trombe-Michel Wall, solar energy, solar radiation, air heating collectors, energy storage

### 1. Introduction

Sunlight is a fundamental factor to be considered in architectural projects. Architects and engineers must know about the apparent sun path to avoid mistakes resulting unnecessarily expensive and energetically inefficient projects. In the South of Brazil this assertion can be corroborated by the need of refrigerating in the summer and heating in the winter of almost every closed ambient in order to achieve the condition of thermal comfort. The usual solution in these cases is the employment of conventional devices, such as air conditioning and fireplaces, with elevated financial and environmental costs.

Along the past few decades the search for the thermal comfort without using conventional forms of energy has resulted in a number of solar houses layouts trying to take the maximum advantage of the available solar energy. The first solar houses were built in the decade of 1930 in the USA (Massachusetts Institute of Technology) and many were built in Europe since early sixties. In Brazil, this subject has received a growing interest from researchers and engineers.

The first challenge in solar energy systems is the thermal storage. For most of the air heating systems using solar energy is during the daytime, period in which the solar energy is available, when heating is less needed. So, when designing such systems, one must find ways to provide energy to the system at night or cloudy periods. One of the storage solutions is by employing high mass (and consequently high thermal capacity) elements in the construction of such devices.

An air heating system, basically a modified Trombe-Michel wall, was built at the facilities of the Solar Energy Laboratory of the Universidade Federal do Rio Grande do Sul. The Trombe-Michel wall is a passive air heating device conceived by French researchers Felix Trombe and Jacques Michel in 1957. The term passive means that no electricity or other form of energy is required than the energy from the Sun.

In its original design, the Trombe-Michel wall is constituted by a massive blackened vertical wall and a glazing, arranged in such a way to form an air gap as shown in Fig. (1). The incoming solar radiation passes through the glass and heats the wall, which in its turn heats the air inside the gap. The air is then pushed, by natural convection, to the inside of the house. The heat absorbed by the air is ready for use. The time needed for the heat to travel across the wall depends on the thermal diffusivity of the concrete, on the difference between internal and external wall surfaces and on the wall thickness.

The paper presents a methodology for determining the daily efficiency of a modified Trombe-Michel wall, henceforth named T-M wall.

### 2. T-M Wall Operation

The studied T-M wall is incorporated to the North façade of the Solar Energy Laboratory of the Universidade Federal do Rio Grande do Sul. The wall is about 16 m wide and is constituted by a solid concrete block with a 24 m<sup>2</sup>,

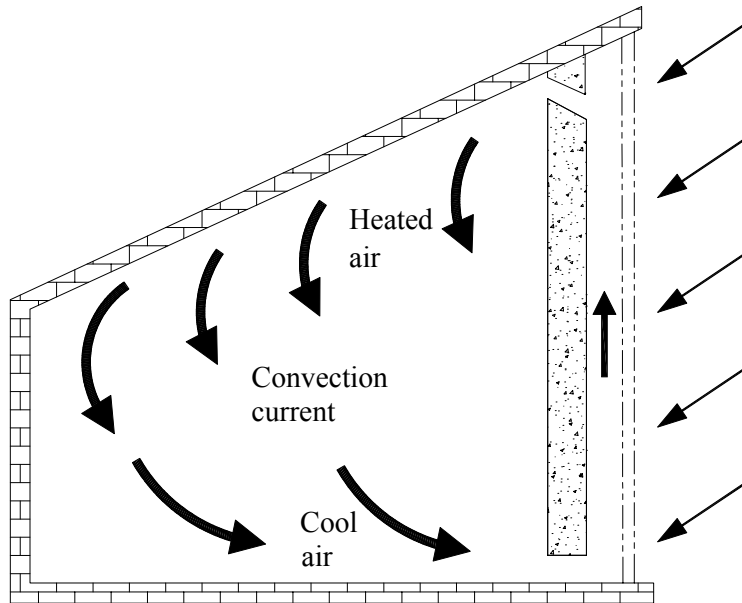


Figure 1. Schematic diagram of the Trombe-Michel wall (from [www.uoregon.edu/~cchatto/ecs\\_case/](http://www.uoregon.edu/~cchatto/ecs_case/)).

50° tilted collection area. The absorbing surface is overlaid with black painted bricks and covered with a double-glazing. Figure (2) shows a cross section of the T-M wall.

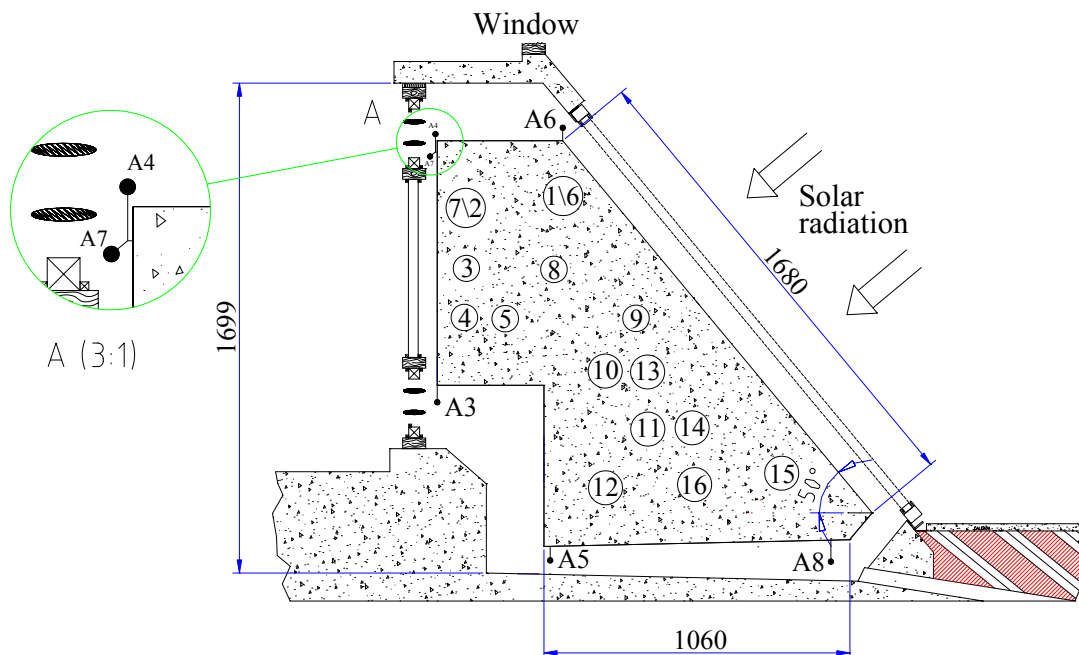


Figure 2. T-M wall cross section showing the position of the temperature sensors (dimensions in mm).

Once in operation, the solar radiation passes through the glazing, being absorbed by the blackened bricks. The absorbed heat is transferred by convection to the air inside the gap. This warmed air is then moved upwards due to buoyancy effects to the top apertures and released to the room, being replaced by the room cool air coming from the bottom apertures.

The physical characteristics of the glass must be known for a better understanding of the T-M wall operation. The glass behaves differently depending on the wavelength of the radiation reaching to its surface. It is very transparent for wavelengths ranging from 0.3  $\mu\text{m}$  to 2.5  $\mu\text{m}$  (solar spectrum) and highly absorptive for wavelengths longer than 5  $\mu\text{m}$  (infrared). Due to this selective property, the glass absorbs the radiation emitted by the collecting surface of the wall. According to the Kirchoff law, being a good absorber means that the glass is also a good emitter in this wavelength

range, so the energy absorbed by the glass and the collecting surface heats the air inside the gap, contributing to a general increase of the temperature of every internal element of the device. Thus the glass, besides letting the solar energy to be transmitted to the collecting surface, acts as a shield for the infrared radiation emitted by this surface and lessens the effects of the wind on the overall convection losses to the outdoor ambient.

The designer of a T-M wall must take into account the thermal diffusivity of the elements that constitute the device. The thermal diffusivity can be defined by Eq. (1):

$$\alpha = \frac{\kappa}{\rho c_p} \quad (1)$$

where  $\alpha$  is the thermal diffusivity,  $\kappa$  is the thermal conductivity,  $\rho$  is the specific mass and  $c_p$  is the specific heat. Materials with higher values of  $\alpha$  will respond quickly to changes in the thermal conditions they are submitted to.

After considering the thermal diffusivity of the different materials, the wall can be sized in such a way that the maximum temperatures of the collecting and the internal surfaces are a few hours lagged. Thus the maximum heat delivery rate to the inside of the room will be reached after the sunset.

### 3. Experimental Assembly

#### 3.1. Description

In order to reduce the complexity of the problem, due to the large number of involved variables, a section of the wall was thermally isolated by a box (1.96 m width x 1.45 m height x 1.10 m depth) made of 50 mm thick expanded polystyrene sheets, attached to the T-M wall inside the room and acting as a calorimeter. This ensures that all of the air flux is trapped inside the box. Thirty plastic bottles filled with water, with a capacity of two liters each and symmetrically arranged on wire racks, were installed inside the box as can be seen in Fig. (3). These bottles serve as a storage mass for measuring the efficiency of the system, simulating the heat absorption that would occur in a larger ambient. Integrated circuit sensors (LM35DZ) were used for monitoring the water temperature. The sensors were installed inside small copper sleeves, attached to the corks of six chosen bottles.

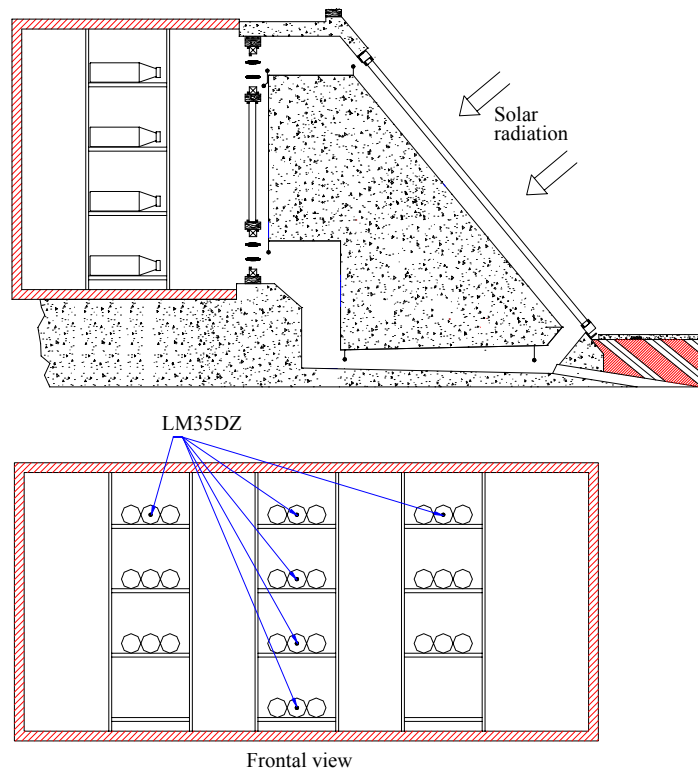


Figure 3. Views of the experimental assembly showing the racks with the water bottles.

Other 16 LM35DZ sensors (to a total of 22) were installed to measure the temperatures of the wall and glazing. Eight platinum resistance sensors (PT100) were used for air temperature measurements, while two photovoltaic pyranometers sensed the solar irradiance.

Those sensors whose position identifier starts with “P” are installed inside the wall. The letter “G” identifies those inside the water bottles. “T1” and “Vi1” measure respectively the absorbing brick surface and internal glass

temperatures. “Ti” and “Te” measure respectively the indoor and outdoor temperatures, while “A3” to “A8” are positioned along the air duct, as shown in Fig. (2).

Table 1. Identification of the temperature sensors with their respective channels and positions.

LM35DZ	Channel	Position
1	201	P1
2	202	P2
3	203	P4
4	210	P5
5	211	P6
6	213	P7
7	217	P8
8	204	P9
9	205	P10
10	206	P12
11	305	P13
12	215	P14
13	207	P15
14	208	P16
15	218	G13
16	219	G14
17	220	G15
18	302	G16
19	303	G17
20	304	G18
21	212	T1
22	216	Vil

PT100	Channel	Position
1	101	Ti
2	102	Te
3	103	A3
4	104	A4
5	105	A5
6	106	A6
7	107	A7
8	108	A8

### 3.2. Characteristics of the Chosen Temperature Sensors

As mentioned before, two types of temperature sensors were employed in the experimental assembly: platinum resistance sensors (PT100) and integrated circuit sensors (LM35DZ).

A PT100 sensor works on the property present by most of the metals of varying their electrical resistance with the temperature. According to Holman, 1971, the platinum sensors satisfy a function in which the resistance varies lineally with the temperature, that is,  $R = f(T)$ :

$$R = R_0(1 + \alpha(T - T_0)) \quad (2)$$

where  $T_0$  is the reference temperature,  $R_0$  is the sensor resistance at the reference temperature and  $\alpha$  is the temperature coefficient. According to Preobrazhenski, 1980, most of the pure metals present positive resistance temperature coefficients, ranging between  $0.004 \text{ }^\circ\text{C}^{-1}$  e  $0.006 \text{ }^\circ\text{C}^{-1}$ .

The main features of platinum resistance sensors are:

- high accuracy;
- high stability of the material and good mechanical resistance;
- high repeatability of the measured values;
- can be used to a long distance with a suitable circuitry;
- more stable and more linear than thermocouples.

All of the PT100 were connected to the data acquisition system with the four-wire method because this technique minimizes the errors introduced by the wires, giving the best results for low resistances.

The main features of the integrated circuit LM35DZ, used to sense the temperatures of the wall and the water inside the bottles, are:

- fine repeatability of the measured values;
- rated for  $0 \text{ }^\circ\text{C}$  to  $100 \text{ }^\circ\text{C}$  range;
- easy installation;
- operates from 4 to 30 Vdc;
- low current drain (less than  $60 \text{ } \mu\text{A}$ );
- low self heating (less than  $0.1 \text{ }^\circ\text{C}$  in still air).



the maximum temperature of the water inside the bottles occurs after 4 to 5 hours after the irradiance peak. It can be noticed also that there is a stratification of the temperatures inside the calorimeter.

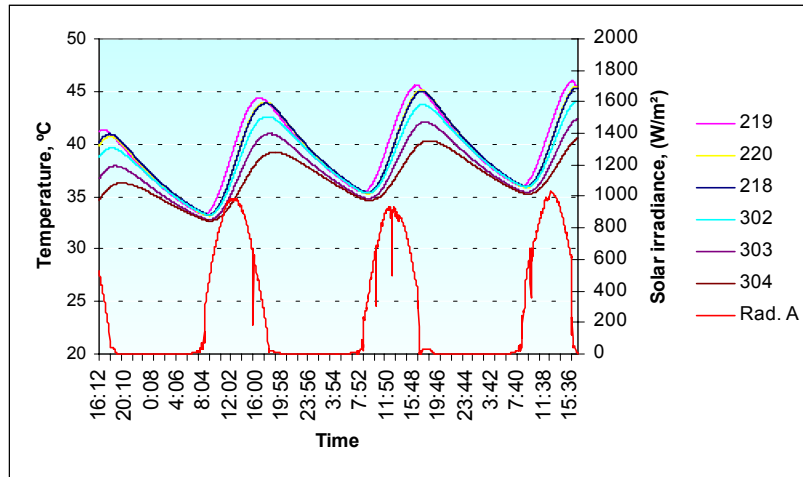


Figure 6. Lag between peaks of temperature and solar irradiance.

This lag between peaks of heat at the absorbing surface and the internal surface is the main effect of the T-M wall, as usually at the moments when the solar radiance is intense there is no crucial need to immediately deliver this heat to the room, since at these periods the ambient air is increased. It is at night, when ambient temperature decreases, that the heat delivered by the T-M wall gains importance. The more heat the wall is able to accumulate during the daytime, the more efficient the system will be, once losses are small.

Some precautions must be considered for the good performance of a T-M wall:

- the covering must be highly transparent to the solar radiation and highly absorptive of the infrared radiation;
- the absorbing surface must be blackened to ensure the maximum energy absorption;
- the top of the T-M wall must be properly insulated to minimize the thermal losses to the ambient;
- the covering must be sealed to avoid admission moisture to the air gap and/or between glasses.

According to Duffie and Beckman, 1991, the efficiency of a solar collector is defined by Eq. (3) the rate between the useful heat removed from the collector and the incident solar radiation over a certain time period.

$$\eta = \frac{\int_{t1}^{t2} Q_u dt}{A_c \int_{t1}^{t2} G_T dt} \quad (3)$$

where  $\eta$  is the efficiency,  $Q_u$  is the useful energy gain,  $G_T$  is the incident solar radiation at the collector plane and  $A_c$  is the collector area. One can notice that the integral is defined over a certain time period. Choosing this integration limits is the core of the problem in the wall efficiency evaluation. If a too short period is selected, the T-M wall efficiency may assume extremely unreal values. In practice, the suitable integration limits will be different for each system, depending on the employed materials, collecting area, wall volume, etc.

In steady state the useful energy transferred to the air  $Q_u$  is defined by the difference between the absorbed solar energy and the thermal losses:

$$Q_u = A_c [S - U_L (T_{pm} - T_a)] \quad (4)$$

where  $S$  is the absorbed energy,  $U_L$  is the T-M wall overall thermal loss coefficient,  $T_{pm}$  is the average temperature of the absorbing surface and  $T_a$  is the ambient temperature. Unfortunately, this kind of system is almost never in steady state so in this case Eq. (4) is of little use.

The methodology to be adopted in this paper consists in calculating the stored heat accumulated by each component of the system according to the following expression:

$$Q_a(n+1) = \sum_{i=1}^4 m_i c_{pi} (T_i^{n+1} - T_i^n) \quad (5)$$

where:

- $Q_a$  is the system current stored heat;
- $m_i$  is the mass of each element  $i$ ;
- $c_{pi}$  is the specific heat of each system component  $i$ ;
- $T_i^{n+1}$  is the current average temperature of each component  $i$ ;
- $T_i^n$  is the previous average temperature of each component  $i$ ;
- $i = 1, 2, 3$  e  $4$  denotes each system component: steel rack, air, concrete and water, respectively.

Equation (5) defines the amount of heat accumulated by the internal elements of the wall over a certain time step, and substitutes the numerator in Eq. (3). The total heat is calculated by summing the accumulated heat in every time step. The equation above was implemented in a computer program written in FORTRAN 90, calculating the accumulated heat from the data registered by the acquisition system. Several time intervals were tested and the time step of 30 minutes was shown to be suitable for the studied T-M wall. The employed constants were obtained from Incropera, 1998.

The nighttime heat loss, the daytime heat gain, the efficiency during the daytime and the daily efficiency were calculated by applying Eq. (5) and integrating the results of the solar irradiance over one day,

## 5. Experimental Results

Figure (7) shows the measured data of the solar irradiance on the T-M wall surface over a sequence of three days (February 26, 27 and 28, 2003). The irradiances were registered by the data acquisition system every two minutes. “Rad. A” represents the external irradiance while “Rad. B” represents the irradiance after the glazing, both at the collector plane. From this data can be calculated the actual double glazing transmittance.

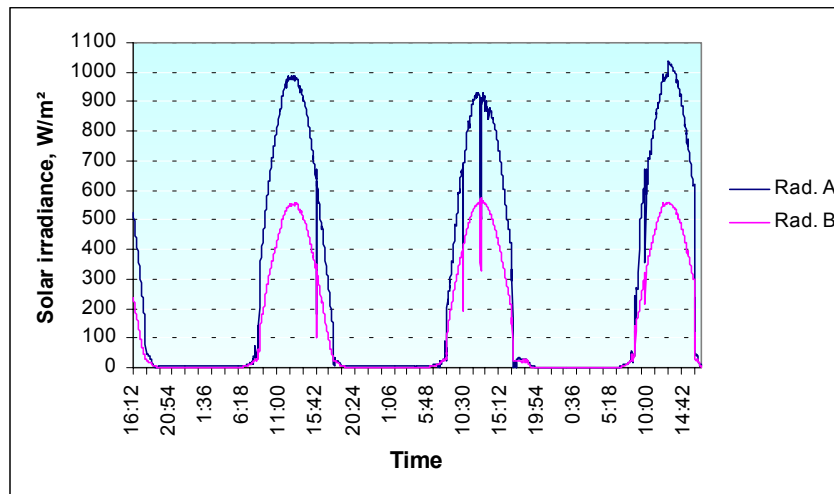


Figure 7. Solar irradiance on the T-M wall surface before and after the glazing.

Figure (8) shows the calculated global solar transmittance through the T-M wall double glazing. One can observe that the maximum solar transmittance (about 55 %) occurs around noon.

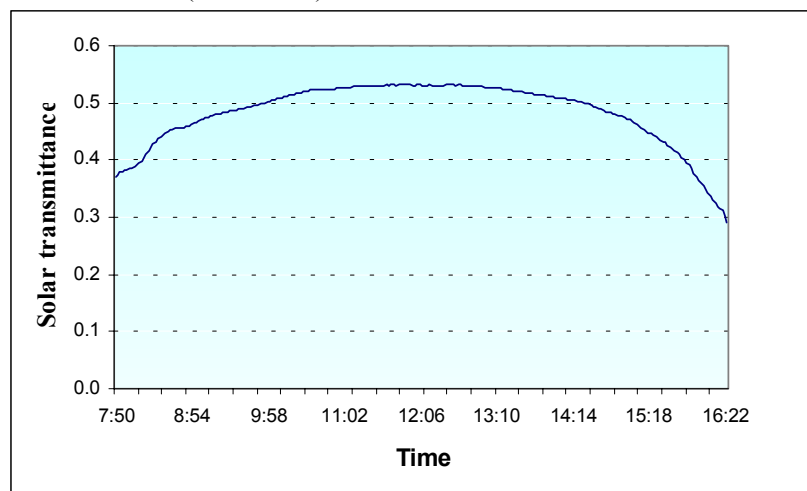


Figure 8. Calculated global solar transmittance through the T-M wall double glazing over a daytime period.

In Fig. (9) are shown the results from the PT100 sensors along the air duct. One can observe the switch between external ( $T_e$ ) and internal ( $T_i$ ) temperatures from day to nighttime, suggesting the good thermal insulation of the Solar Energy Laboratory. In this graphic can be also observed that the maximum air temperature is delayed by two to three hours from the solar irradiance peak. All the monitored points of the duct presented similar behavior. Sensor “106”, installed just after the absorbing surface and the first to be reached by the heated air flux, registered the maximum air temperature of around 60 °C.

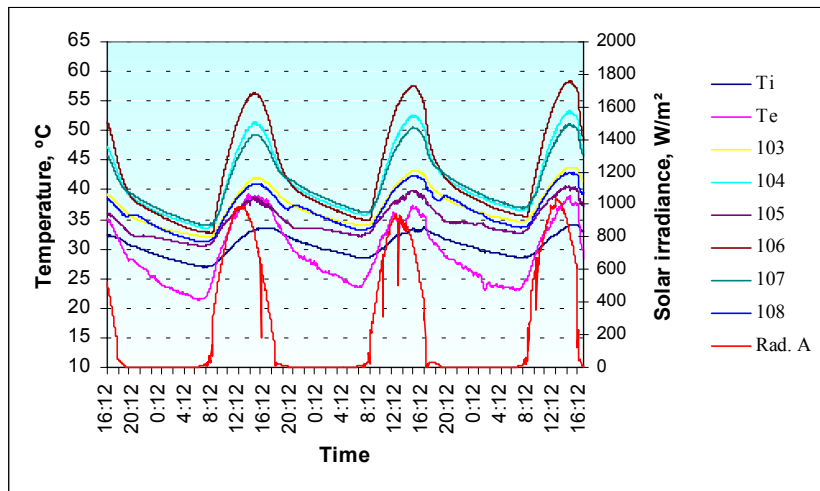


Figure 9. Temperatures inside the air duct of the T-M wall and external solar irradiance.

The graphic in Fig. (10) was obtained from Eq. (6) with a time step of 30 minutes, showing the effects of the accumulated heat and the solar irradiance over the same sequence of three days (February 26, 27 and 28, 2003). The accumulated heat curve was smoothed in order to facilitate the visualization. A lag of four to five hours in accumulated heat peak can be observed, indicating that the wall continues to deliver heat hours after the sunset.

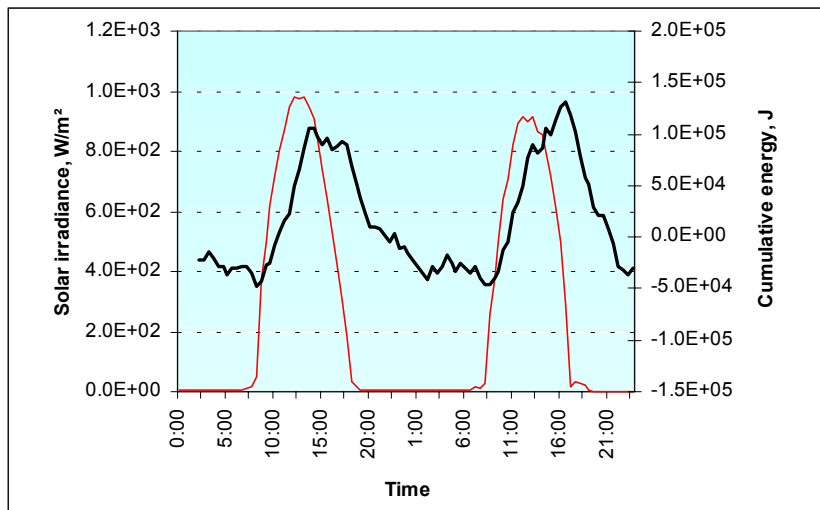


Figure 10. Delay between the solar irradiance and the accumulated heat delivered by the wall.

Table (2) presents the results for the daytimes of the same three days sequence, showing the heat accumulated by each system component. It can be observed that most of the heat is stored in the concrete. The average daytime efficiency was about 25 %.

Table 2. Solar radiation and heat accumulated by each component in the daytime periods.

Date	Period	Solar radiation (J)	Cumulative water (J)	Cumulative rack (J)	Cumulative concrete (J)	Cumulative air (J)	Efficiency
26/02/03	7:00 - 18:22	6.74E+07	4.45E+05	4.43E+03	1.35E+07	1.82E+04	21%
27/02/03	6:10 - 18:10	5.82E+07	2.99E+05	4.43E+03	1.60E+07	1.45E+04	28%
28/02/03	6:30 - 16:20	6.05E+07	4.94E+05	1.20E+02	1.51E+07	1.82E+04	26%

Table (3) shows the nighttime results of the same three days sequence. A significant oscillation of the total thermal losses from night to night can be observed.

Table 3. Nighttime thermal losses of each T-M wall component.

Date	Period	Solar radiation (J)	Cumulative water (J)	Cumulative rack (J)	Cumulative concrete (J)	Cumulative air (J)	Total loss
26/02/03	18:30-06:30	0.00E+00	-7.25E+04	4.43E+03	-6.61E+07	1.09E+04	-6.61E+07
27/02/03	18:00-07:00	0.00E+00	-1.23E+05	4.43E+03	-5.81E+07	1.82E+03	-5.82E+07
28/02/03	18:00-06:00	0.00E+00	1.68E+05	1.30E+03	-1.48E+07	-1.27E+04	-1.46E+07

Table (4) shows the calculated daily efficiencies. The 24 h intervals started at 12 pm. It was observed that the daily efficiency is heavily influenced by the initial time. Depending on the chosen initial time the efficiency calculation will vary between 25 % e 14 %.

Table 4. Daily efficiencies of the T-M wall.

Date	Period	Daily efficiency
26	24 hours	14%
27	24 hours	15%
28	24 hours	16%

One of the reasons of the increased thermal losses at the first night period was due to the lower indoor and outdoor ambient temperatures at nighttime, as can be seen in Fig. (11).

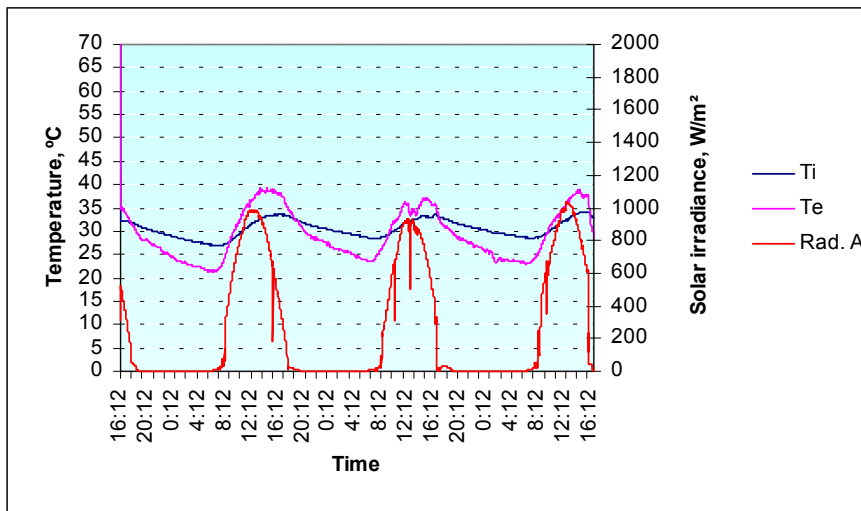


Figure 11. Measured values of the solar irradiance and internal and external temperatures for the analyzed three days sequence.

Other sources of increased thermal losses are insufficient insulation of the T-M wall covering and the presence of a cold air mass, which may result in a significant increase of the convection losses through the T-M wall glazing.

## 6. Conclusion

The present work presented and discussed the characteristics of a residential passive air heating system. A computerized data acquisition system with 30 temperature and two irradiance sensors was utilized. Due to the complexity of the problem an alternative method for calculating the T-M wall daily efficiency was proposed. It was noticed that the daily efficiency is heavily influenced by the initial time.

A 4 to 5-hours lag between the peak of the solar irradiance and the peak of the accumulated heat was observed.

This work will be continued with the collection of more experimental data looking for determining a correlation between operation temperature and efficiency.

## **7. Acknowledgements**

This work was supported by Conselho de Desenvolvimento Científico e Tecnológico - CNPq.

## **8. References**

- Duffie, J. A. and Beckman, W. A., 1991, "Solar Engineering of Thermal Processes", Ed. John Wiley & Sons, New York, USA, pp. 251-252
- Givoni, B., 1998, "Climate Consideration in Building and Urban Design", VN Reinhold, New York, 464 p, pp. 162-163.
- Holman, J. P., 1971, "Experimental Methods for Engineers", McGraw-Hill Book Company, New York
- Incropera, F. P. and Dewitt, D. P., 1998, "Fundamentos de Transferência de Calor e de Massa", LTC – Editor Livros Técnicos e Científicos, Rio de Janeiro, Brazil, pp. 448-465.
- Preobrazhenski, V. P., 1980, "Mediciones Termotécnicas y Aparatos para Efectuarlas", Mir, Moscow, pp. 208-215, Vol. I, pp. 244-248.